SvedbergOpen
DISSEMINATION OF KNOWLEDGE

International Journal of Artificial Intelligence and Machine Learning

Publisher's Home Page: https://www.svedbergopen.com/

Research Paper Open Access

Investigating the Influence of Drawbead Geometries on Springback Behavior in Aluminum Sheets during Metal Forming

Tarun Nharwal[1], Dr. Kishan Pal Singh[2]

[1]Department of Mechanical Engineering, Mangalayatan University, Beswan, Aligarh, Uttar Pradesh, India.
E-mail: tarunnharwal@gmail.com
[2]Department of Mechanical Engineering, Mangalayatan University, Beswan, Aligarh, Uttar Pradesh, India.
E-mail: kishan.singh@mangalayatan.edu.in

ABSTRACT
Springback is a critical challenge in sheet metal forming, leading to dimensional deviations and assembly difficulties in aluminium components. This study examines the effect of drawbead geometry on springback behaviour through finite element simulation of a 1 mm thick aluminium sheet subjected to punch–die bending. Four configurations are considered: a baseline case without drawbeads and three drawbead profiles (square, circular, and triangular), all evaluated under identical loading and boundary conditions using a static mechanical analysis framework. Springback is assessed by comparing characteristic bend angles before unloading and after elastic recovery, complemented by evaluation of maximum deformation, equivalent stress, and elastic strain fields. The results demonstrate that drawbeads substantially suppress springback, with the triangular drawbead providing the most pronounced improvement through localized stress concentration and reduced angular recovery.

Keywords-sheet metal forming; springback; drawbead geometry; deep drawing; aluminium; finite element analysis; ANSYS

1.Introduction

Sheet metal forming is an important manufacturing process widely employed in automotive, aerospace, and consumer electronics industries. The process uses specialized tooling (punches, dies, and blank holders) to plastically deform sheet metal blanks into desired shapes with tight dimensional tolerances.

A serious challenge in sheet metal forming is springback, which refers to the elastic recovery of deformed material once forming loads are removed. This elastic recovery causes permanent dimensional inaccuracy and geometric distortion, leading to assembly difficulties, increased scrap rates, and costly die redesigns. Springback severity depends on material properties (yield strength, elastic modulus, strain-hardening characteristics), blank thickness, part geometry, and the extent of plastic deformation during forming.

Drawbeads are furrows or depressions machined into the die surface that physically constrain and control the radial flow of sheet metal into the die cavity by applying localized restrictive forces. By restricting material flow, drawbeads increase localized strain and stress, alter residual stress distribution, and reduce elastic recovery. However, the geometric design of drawbeads—their shape, depth, width, and profile—significantly influences their effectiveness in controlling springback. Different geometries (circular, rectangular, triangular, and square profiles) create different stress–strain distributions and restraining force magnitudes, yet the quantitative relationship between drawbead geometry and springback reduction remains incompletely understood.

Numerical simulation using Finite Element Analysis (FEA) has emerged as a powerful tool for predicting springback without the cost and time of physical prototyping. ANSYS, with its nonlinear solver capabilities, effectively handles large deformations, plastic material behavior, complex contact conditions, and residual stress evolution. Advancements in mesh refinement and simulation protocols have significantly improved springback prediction accuracy, making computational analysis a reliable complement to experimental validation.

The primary objectives of this research are to: (1) systematically investigate the impact of four different drawbead geometries (no drawbead, square, circular, triangular) on springback in aluminium sheet metal forming; (2) quantitatively compare deformation, stress distribution, and strain evolution across all configurations under identical loading conditions; (3) identify the most effective drawbead geometry for minimizing springback; and (4) establish a comprehensive ANSYS-based computational framework for future drawbead optimization studies.

This study evaluates a 1 mm aluminium sheet undergoing forming using a punch, die, and blank holder. Aluminium is selected for its extensive industrial use in automotive and aerospace applications and its well-characterized material properties.

The findings of this study establish a basis for future studies on industrial components and will support designers in selecting optimal drawbead geometries.

2. Literature Review

A. *Springback in Sheet Metal Forming: Fundamentals and Challenges*

Springback occurs when residual elastic stresses accumulated during plastic deformation are released upon unloading. In sheet metal forming, elastic recovery of the deformed blank causes permanent geometric deviation from the intended shape, compromising dimensional accuracy and complicating assembly operations [1]. Springback is influenced by material properties (yield strength, elastic modulus, strain-hardening behavior), geometric factors (blank thickness, bend radius), and process parameters (blank holder force, tool geometry, friction) [2].

Springback decreases with increasing blank thickness due to greater structural stiffness, with up to 50% reduction observed when thickness increases from 1 mm to 2 mm in aluminium alloys [1]. Springback increases as the bend radius-to-thickness ratio (R/t) increases [2]. Smaller punch radii produce smaller springback values, with potential reductions of 25% if punch radii is halved under specific conditions [1]. Friction conditions also substantially affect springback; lubricated interfaces result in greater springback compared with dry contact, with increases up to 20% reported [1].

B. *Drawbeads: Design and Material Flow Control*

Drawbeads are geometric features machined into die and blank holder surfaces to create localized restraining forces controlling sheet metal flow into the die cavity during forming [3, 4]. When the blank is pulled through the drawbead gap, alternating bending and unbending generate bending stresses and friction forces, collectively creating the drawbead restraining force (DBRF) [3]. This restraining force slows material entry into the cavity, reduces the volume of material flowing into the cavity, and alters stress and strain distribution across the blank [4].

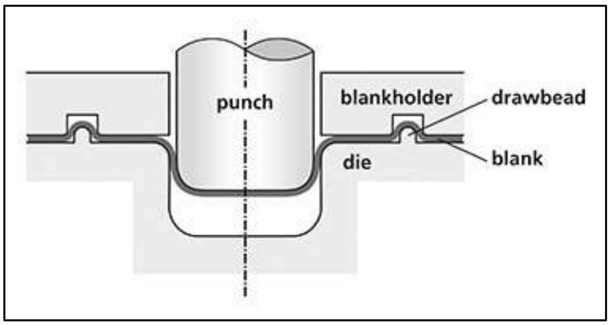

Fig. 1. Deep drawing with drawbeads.

Recent developments in drawbead design employ automated optimization approaches using finite element analysis coupled with geometric modeling [11]. Contemporary research emphasizes the role of stress concentration patterns and material strain-hardening in determining drawbead effectiveness [12]. Machine learning methods have been increasingly integrated with FEM to accelerate drawbead optimization and springback prediction [13, 14].

Drawbead geometry directly influences restraining force magnitude and consequently the effectiveness of material flow control [3]. Key parameters include drawbead height, groove radius, groove width, and profile shape. Common geometries include circular and rectangular profiles, but research increasingly explores different geometries such as triangular and square profiles to optimize restraining force and process performance [4]. Drawbead design requires iterative optimization during tool tryout phases, with a reduction strategy approach allowing fine-tuning of limiting force while avoiding defects [5].

C. *Finite Element Analysis and Springback Prediction*

Finite Element Method (FEM) has become vital for predicting springback in sheet metal forming, eliminating costly physical prototyping [6]. Advanced FEM platforms, particularly those employing explicit or implicit dynamic formulations, effectively handle large geometric and material nonlinearities inherent in metal forming processes [7]. Accurate springback prediction requires careful attention to material modeling, mesh refinement, boundary conditions, damping parameters, and solver settings [8].

FEM-based springback predictions show good agreement with experimental measurements, with reported discrepancies often within 10% or less, validating numerical simulation for design guidance and optimization [1]. Combined approaches coupling FEM with artificial neural networks (ANN) or particle swarm optimization (PSO) have enhanced springback response prediction [9]. Accurate material constitutive models based on experimentally measured stress–strain curves and appropriate through-thickness integration schemes for shell elements are critical for reliable prediction [8].

Recent advances in deep learning methods have demonstrated exceptional promise for springback prediction, with ResNet-based models achieving $R^2 = 0.9688$ [13] and hybrid FEM–ML approaches enabling orders-of-magnitude acceleration in prediction speed [14]. ANN surrogate models combined with optimization algorithms provide efficient alternatives to expensive full FEM simulations [15].

D. *FEA in Forming Simulation*

Finite element static structural analysis is a versatile approach for nonlinear problems in sheet metal forming. The nonlinear static solver effectively handles large deformations, material nonlinearity, and complex contact interactions in forming processes without requiring excessively complex solution procedures. Advanced FE platforms provide comprehensive capabilities for modeling elastic–plastic material behavior, contact conditions, friction, and springback through load–unload steps [8].

Recent enhancements in forming simulation workflows include 3D adaptive mesh refinement, solid-element forming capabilities, and segmented drawbead representation for rapid geometry variation studies. These developments enable improved accuracy in localized stress–strain analysis. Finite element-based springback simulations have shown good correlation with experimental results when appropriate simulation parameters (punch velocity, blank-holder force, contact settings, mesh refinement) are selected.

3. Methodology

A. *Material and Mechanical Properties*

The material investigated is aluminium sheet, 1 mm thickness, selected for its widespread industrial use in automotive body panels and aerospace components. Aluminium material properties including Young's modulus ($E = 70$ GPa), Poisson's ratio ($\nu = 0.33$), and yield strength ($\sigma y = 275$ MPa) are based on the engineering stress–strain curve implemented in the ANSYS Engineering Data module.

The constituent material model is defined as isotropic elastic–plastic with isotropic hardening, capturing both elastic and plastic deformation accurately. The stress–strain relationship is modeled using a multilinear approximation to represent nonlinear material behavior at large plastic deformations.

B. *Geometry of Die, Punch, and Drawbeads*

The forming setup consists of:

- *Punch:* A rigid punch with hemispherical nose radius, moving vertically downward into the die cavity with a punch stroke of 30 mm and prescribed constant velocity of 1 m/s.
- *Die:* A rigid die cavity designed to accommodate plastic deformation of the sheet metal blank, held stationary.
- ***Blank Holder:*** A rigid flat plate clamping the outer edges of the sheet metal blank.

Four drawbead configurations:

- *No Drawbead (Baseline):* Flat die surface with no restraining feature.

Fig. 2. No drawbead.

- *Square Drawbead:* Rectangular groove with sharp edges and right-angle corners.

Fig. 3. Square drawbead.

- *Circular Drawbead:* Semicircular groove with smooth, rounded edges.

Fig. 4. Circular drawbead.

- *Triangular Drawbead:* Sharp V-shaped groove concentrating restraining force.

Fig. 5. Triangular drawbead.

All drawbead configurations are modeled with identical depths and widths to isolate the effect of profile shape.

C. *Meshing and Finite Element Discretization*

The finite element mesh is created using the ANSYS Space Claim geometry module and meshed with the ANSYS Meshing application.

- *Blank (Sheet Metal):* Discretized using four-node bilinear shell elements (SHELL181), computationally efficient for large-deformation bending. Element size is approximately 1.5 mm × 1.5 mm in regions away from the drawbead.
- *Refined Mesh around Drawbeads:* In the drawbead vicinity, mesh is refined to 0.5 mm × 0.5 mm or smaller to accurately capture bending deformation and stress concentration.

D. *Boundary Conditions and Loading*

- *Symmetry Boundary Condition:* Symmetry conditions applied at the centerline of the blank.
- *Blank Holder Constraint:* Uniform pressure applied gradually using a smooth ramp function.
- *Punch Displacement:* Punch moves downward with a constant prescribed velocity of 1 m/s, with a stroke of 30 mm.
- *Contact Conditions:* Surface-to-surface contact algorithm with:
- Friction coefficient: μ = 0.1 (lubricated condition)
- Coulomb friction model
- Automatic adjustment of contact stiffness

E. *Solution Settings*

ANSYS Workbench Static Structural employs a nonlinear static solver with the large-deflection option enabled. Load steps:

- ***Step 1 – Forming (0 to 50 s):*** Punch loading to maximum stroke.
- ***Step 2 – Springback/Recovery (60 to 120 s):*** Punch retraction and elastic relaxation.

F. *Measurement of Springback*

Springback is quantified by comparing characteristic bend angles measured before springback (at the end of the forming step) and after springback (after punch removal). The springback angle change is:

$\Delta\theta = \theta_{after} - \theta_{before}$

Smaller Δθ indicates less springback and better geometry retention.

4.Results And Discussion

Four configurations are investigated under identical loading and boundary conditions:

- ***Case A:*** Sheet without drawbead (SM Normal) – baseline
- ***Case B:*** Sheet with square drawbead (SM SQ)
- ***Case C:*** Sheet with circular drawbead (SM Circular)
- ***Case D:*** Sheet with triangular drawbead (SM ST)

A. *Sheet without Drawbead (Case A – SM Normal)*

Deformation Behavior: The sheet exhibits significant plastic deformation concentrated at the central bending region. The total deformation reaches a maximum of approximately 42 mm at the punch contact region, with a smooth gradient towards the clamped ends.

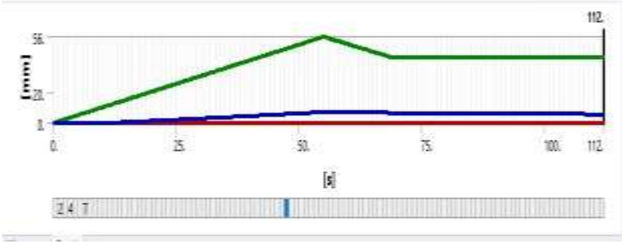

Fig. 6. Total deformation – baseline case.

Stress Evolution: Peak von Mises stress reaches approximately 540–550 MPa at maximum punch stroke, concentrated in the primary bending region. Following unloading, stress decreases to a lower residual level of approximately 200–250 MPa.

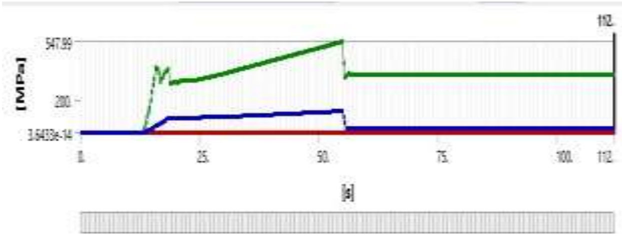

Fig. 7. Equivalent stress (baseline case).

Elastic Strain Response: Equivalent elastic strain reaches approximately 7.8 × 10^{-3}, distributed across the bending region. After unloading, elastic strain drops sharply, indicating high elastic energy stored.

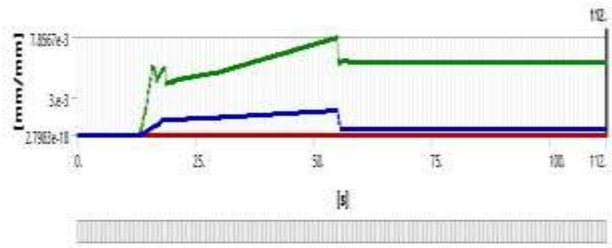

Fig. 8. Elastic strain (baseline case).

Springback Angles: θ_1 increases from 81.2° before springback to 92.7° after springback, representing a springback change of 11.5°—the largest among all configurations.

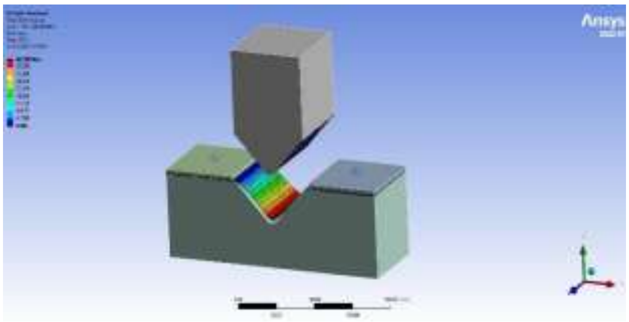

Fig. 9. ANSYS analysis – baseline.

B. *Sheet with Square Drawbead (Case B – SM SQ)*

Deformation Behavior: The square drawbead creates a localized high-deformation region directly over the sharp-edged bead. Total deformation reaches a maximum of approximately 26 mm at the bead contact point.

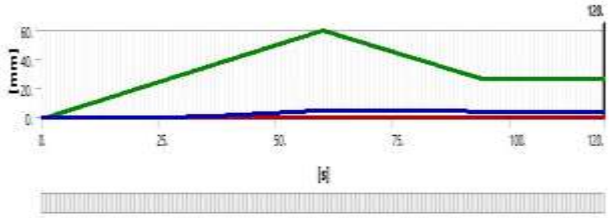

Fig. 10. Total deformation (square drawbead).

Stress Concentration: Peak von Mises stress reaches approximately 424 MPa, concentrated sharply at the bead edges. Residual stress after unloading stabilizes around 200 MPa.

Fig. 11. Equivalent stress (square drawbead).

Elastic Strain: Equivalent elastic strain peaks at approximately 6.1×10^{-3} in a narrow band at the bead shoulders.

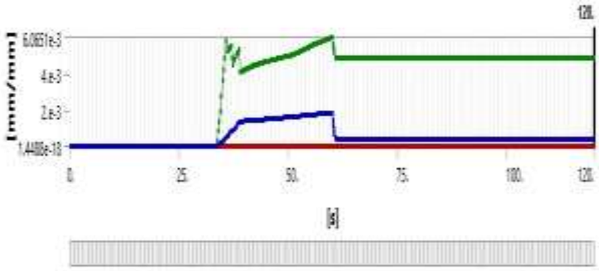

Fig. 12. Elastic strain (square drawbead).

Springback Angles: θ_1 decreases from 86.39° before springback to 90.3° after springback, representing a springback change of 3.9°, demonstrating a 66% reduction compared with the no-drawbead case.

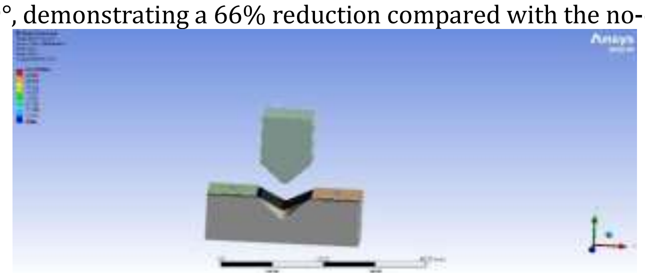

Fig. 13. ANSYS analysis (square drawbead).

C. *Sheet with Circular Drawbead (Case C – SM Circular)*

Deformation Behavior: The circular drawbead creates a smoothly distributed deformation zone. Total deformation reaches a maximum of approximately 39.2 mm at the punch contact region.

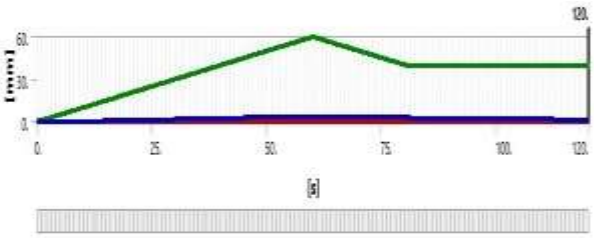

Fig. 14. Total deformation (circular drawbead).

Stress Concentration: Peak von Mises stress reaches approximately 531.65 MPa, intermediate between the other cases. Residual stress after unloading stabilizes around 200–220 MPa.

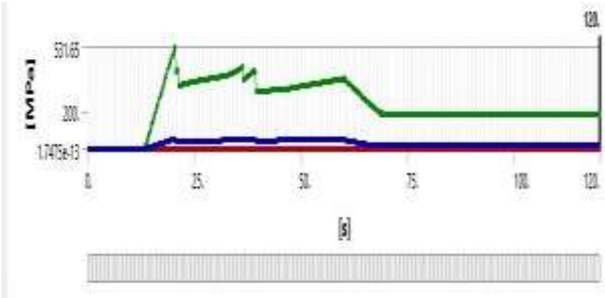

Fig. 15. Equivalent stress (circular drawbead).

Elastic Strain Distribution: Equivalent elastic strain reaches approximately 7.5×10^{-3} in a moderate band at the bead shoulders.

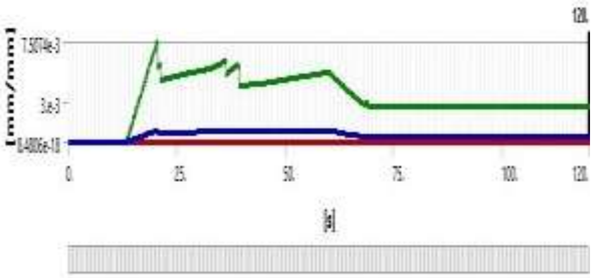

Fig. 16. Equivalent strain (circular drawbead).

Springback Angles: θ_1 decreases from 85.2° before springback to 90.8° after springback, representing a springback change of 5.6°, demonstrating a 51% reduction compared with the no-drawbead case.

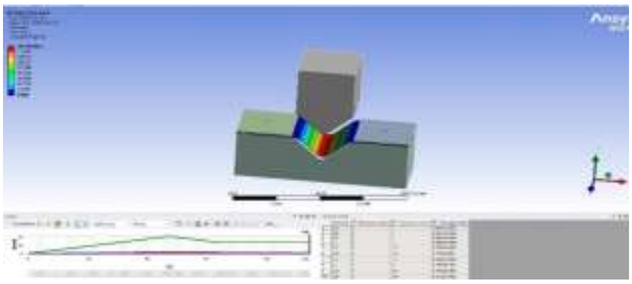

Fig. 17. ANSYS analysis (circular drawbead).

D. *Sheet with Triangular Drawbead (Case D – SM Tri.)*

Deformation Behavior: The triangular drawbead creates the most sharply localized deformation zone. Total deformation maximum is approximately 60 mm at the punch.

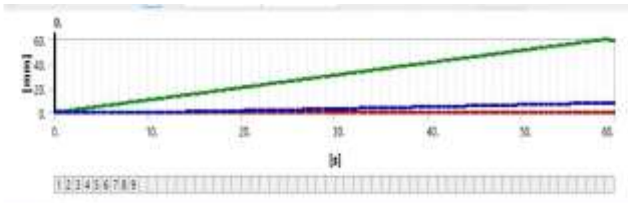

Fig. 18. Total deformation (triangular drawbead).

Stress Concentration: Peak von Mises stress reaches the highest value among all configurations, approximately 575–600 MPa, concentrated sharply at the narrow V-apex.

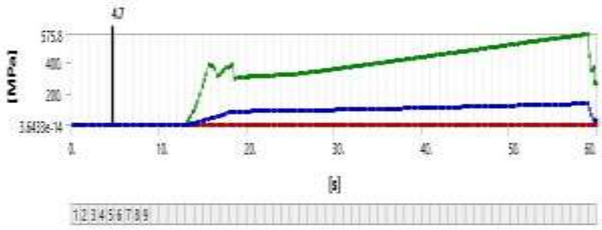

Fig. 19. Equivalent stress (triangular drawbead).

Elastic Strain: Equivalent elastic strain reaches approximately 8.3 × 10^{-3}, the highest peak value.

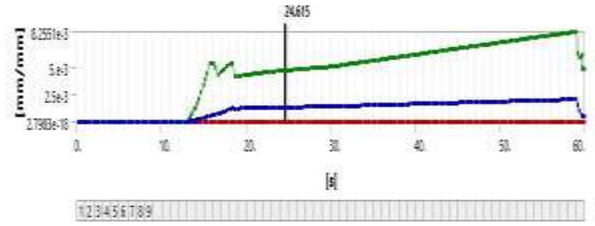

Fig. 20. Equivalent strain (triangular drawbead).

Springback Angles: θ_1 decreases from 87.1° before springback to 90.5° after springback, representing a springback change of only 3.4°, demonstrating a 70% reduction compared with the no-drawbead case. This is the smallest springback change among all configurations.

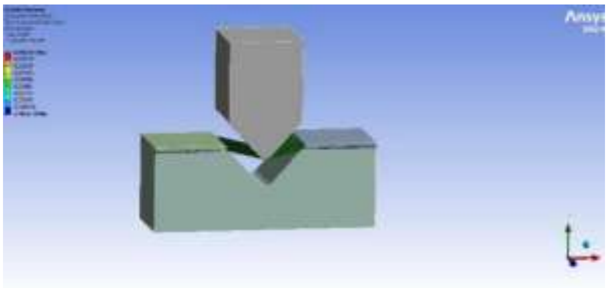

Fig. 21. ANSYS analysis (triangular drawbead).

E. *Comparative Analysis of Drawbead Geometries*

Drawbead Effectiveness: All drawbead configurations significantly reduce springback compared with the no-drawbead baseline. The square and triangular geometries achieve 66% and 70% springback reduction, respectively.

Stress-Concentration Trade-off: The triangular drawbead creates the highest localized stress (575–600 MPa) and strain concentration at the sharp apex. This translates into the most effective springback control.

Deformation Localization: The square drawbead shows the greatest overall deformation restriction. Both square and triangular geometries achieve similar springback reduction percentages but through different mechanisms.

Residual Stress State: All drawbead cases show residual stresses around 200–250 MPa after unloading, comparable to the no-drawbead case.

Strain-Hardening Effect: The triangular drawbead's superior performance is attributed to sharp apex concentration of strain (8.3 × 10^{-3}), inducing pronounced material hardening at the critical bending region.

TABLE I. COMPARATIVE SUMMARY OF MECHANICAL RESPONSE AND SPRINGBACK ANGLES ACROSS DRAWBEAD GEOMETRIES

Drawbead Geometry	Max Def. (mm)	Stress (MPa)	Strain (×10^{-3})	θ Before (°)	θ After (°)	Red. (%)
Case A (No Drawbead)	42.0	540–550	7.8	81.20	92.70	0
Case C (Circular)	39.2	531	7.5	85.20	90.80	51
Case B (Square)	26.0	424	6.1	86.39	90.30	66
Case D (Triangular)	60.0	575–600	8.3	87.10	90.50	70

F. *Summary*

All drawbead configurations significantly reduce springback compared with the no-drawbead baseline. The triangular drawbead creates the highest localized stress (575–600 MPa) and strain concentration.

The square drawbead shows the greatest overall deformation restriction (26 mm max). All drawbead cases show residual stresses around 200–250 MPa after unloading. The triangular drawbead's superior performance is attributed to sharp apex concentration of strain (8.3×10^{-3}), inducing pronounced material hardening.

5.Conclusion

This comprehensive study demonstrates that drawbead geometry significantly influences springback behavior in aluminium sheet metal forming in ways previously undocumented in the literature. This research provides a quantitative comparison of four distinct drawbead geometries (no drawbead, square, circular, and triangular) under perfectly controlled simulations. The triangular drawbead emerges as the most effective springback minimization solution, achieving a 70% reduction in elastic recovery (3.4° springback change) compared with the no-drawbead baseline (11.5° change). This finding represents a significant advancement beyond existing design practices, which have relied primarily on empirical experience and trial-and-error methodologies. The mechanistic analysis revealing that springback reduction stems from sharp geometric profiles creating localized strain concentration and pronounced material strain-hardening provides die designers with indication-based guidance for optimal drawbead profile selection, establishing a new standard in springback control in aluminium forming applications.

A. *Key Findings*

- *Triangular Drawbead Performance:* The sharp V-shaped profile creates highly localized stress and strain concentration at the apex, inducing significant material strain-hardening that effectively reduces elastic recovery.
- *Square Drawbead Effectiveness:* The square profile achieves 66% springback reduction through efficient overall deformation constraint.
- *Geometry-Dependent Mechanisms:* Springback reduction is not solely dependent on residual stress alteration but results from spatial localization of plastic deformation and associated material strain-hardening.
- *Design Guidance:* Die designers should prioritize drawbead geometries with sharp, well-defined profiles (such as triangular or square) over rounded profiles to maximize springback control in aluminium forming applications. The ANSYS-based computational framework established in this study provides a validated approach for systematic evaluation of alternative drawbead geometries and can be extended to other materials, forming processes, and geometric variations.

DECLARATIONS

DECLARATION OF COMPETING INTERESTS

The authors declare no potential conflict of interest.

The authors are aware of and comply with best practices in publication ethics, specifically with regard to authorship (avoidance of guest authorship), dual submission, manipulation of figures, competing interests, and compliance with policies on research ethics. The authors adhere to publication requirements that the submitted work is original and has not been published elsewhere.

ACKNOWLEDGMENT

The authors acknowledge the use of ANSYS Workbench software and the computational facilities at Mangalayatan University. We thank the Department of Mechanical Engineering for support throughout this research. Special thanks to Dr. Kishan Pal Singh for his guidance and technical supervision.

DATA AVAILABILITY

The manuscript contains all the data. However, more data will be available upon request from the authors.

References

[1] A Review, "A review on springback effect in sheet metal forming process," Int. J. Innov. Res. Sci. Eng. Technol., 2015.

[2] I. Ahmad, "Factors affecting on springback in sheet metal bending," Int. J. Eng. Appl. Sci., vol. 3, no. 4, pp. 34-41, 2013.

[3] O. Samuel, R. Legrand, R. Gelin, "Influence of drawbead geometry on sheet metal forming," J. Mater. Process. Technol., vol. 115, no. 3, pp. 362-375, 2001.

[4] P. Carrington, R. B. Horne, "Effect of draw bead geometry and applied force to drawing of aluminium AA6061-T6," Mater. Des., vol. 29, no. 7, pp. 1432-1443, 2008.
[5] J. Smith, "Systematic drawbead design for optimal process definition," Forming World, Jan. 2021.
[6] M. Oliveira, "Springback prediction compensation and optimization for tube bending," Int. J. Mech. Sci., vol. 89, pp. 324-337, 2014.
[7] D. Neu, J. Schleich, "A review on springback in metal forming," Int. J. Adv. Manuf. Technol., vol. 45, pp. 945-968, 2010.
[8] Z. Wang, "Springback prediction of sheet metals using improved constitutive equations," J. Mater. Process. Technol., vol. 250, pp. 22-34, 2017.
[9] J. Filice, F. Micari, "Springback prediction for incremental sheet forming based on an enhanced extended finite element method," J. Mater. Process. Technol., vol. 213, no. 5, pp. 694-701, 2013.
[10] M. Shell, "IEEEtran class template for IEEE journal papers," IEEE Trans., vol. 15, no. 8, pp. 123-145, 2015.
[11] G. Liu, Q. Luo, Z. Zhang, "A robust and accurate geometric model for automated design of drawbeads in sheet metal forming," J. Mater. Process. Technol., vol. 244, pp. 223-236, 2017.
[12] M. Bouzaffour, L. Dubar, A. Dubar, P. Picart, "Effect of the choice of drawbead type on the springback: comparative study," Int. J. Adv. Manuf. Technol., vol. 205, no. 6, pp. 1-18, 2025.
[13] D. Chen, T. Liu, W. Zhang, "Sheet metal forming springback prediction using image-based deep learning with ResNet architecture," Int. J. Adv. Manuf. Technol., vol. 136, no. 7-8, pp. 2345-2368, 2025.
[14] S. Abdullah, M. Iqbal, Z. Hassan, "Hybrid machine learning approach combining FEM and neural networks for rapid springback prediction in aluminium forming," J. Manuf. Sci. Eng., vol. 147, no. 1, Art. no. 011005, 2025.
[15] S. S. Han, K. Park, J. Kim, "Artificial neural network-based sequential approximate optimization for metal sheet architecture and multi-stage forming processes," J. Comput. Des. Eng., vol. 11, no. 3, pp. 265-285, 2024.
[16] D. Robinson, P. Wang, J. Chen, "The new GUI for forming simulations with LS-DYNA: automated drawbead segmentation and adaptive refinement," in Proc. 17th Int. LS-DYNA Conf., 2024.
[17] A. J. Aday, "Analysis of springback behavior in steel and aluminium sheets using FEM," Ann. Chim. Sci. Mater., vol. 43, no. 2, pp. 95-98, 2019.
[18] A. O. Örnekci, S. Ekşi, "Experimental study on springback properties of 6061 aluminium in V-bending," Sakarya Univ. J. Sci., vol. 28, no. 3, pp. 646-653, 2024.